Phase transition from straight into twisted vortex lines in dipolar Bose–Einstein condensates

2009 New J. Phys. 11 055012

(http://iopscience.iop.org/1367-2630/11/5/055012)

New Journal of Physics
The open-access journal for physics

Phase transition from straight into twisted vortex lines in dipolar Bose–Einstein condensates

M Klawunn[1] **and L Santos**
Institut für Theoretische Physik, Leibniz Universität Hannover, Appelstr. 2, D-30167 Hannover, Germany
E-mail: klawunn@itp.uni-hannover.de

New Journal of Physics **11** (2009) 055012 (11pp)
Received 25 November 2008
Published 14 May 2009
Online at http://www.njp.org/
doi:10.1088/1367-2630/11/5/055012

Abstract. The non-local nonlinearity introduced by the dipole–dipole interaction plays a crucial role in the physics of dipolar Bose–Einstein condensates. In particular, it may distort significantly the stability of straight vortex lines due to the rotonization of the Kelvin-wave spectrum. In the present paper, we analyze this instability, showing that it leads to a second-order-like phase transition from a straight vortex line into novel helical or snake-like configurations, depending on the dipole orientation.

Contents

1. Introduction 2
2. Dipolar BEC in an optical lattice: effective model 3
3. Kelvin-wave instability of a straight vortex line 5
4. Helical vortices 7
5. Snake-like vortices 9
6. Conclusions 10
Acknowledgments 10
References 10

[1] Author to whom any correspondence should be addressed.

1. Introduction

The physics of ultra-cold atomic and molecular gases is crucially determined by the inter-particle interactions. Typical experiments in quantum gases have so far studied particles that interact dominantly via short-range isotropic potentials. At the very low energies involved in these experiments, such interactions are characterized by a single parameter, namely the s-wave scattering length. However, a new generation of recent experiments is opening a fascinating new research area, namely that of dipolar gases, for which the dipole–dipole interaction (DDI) plays a significant or even dominant role. These experiments include, on the one hand, those dealing with the DDI effects due to magnetic dipoles in degenerate atomic gases, as is the case of recent exciting experiments in chromium Bose–Einstein condensates (BECs) [1] and rubidium spinor BECs [2]. On the other hand, recent experiments on the creation of heteronuclear molecules in the lowest vibrational states [3], although not yet brought to quantum degeneracy, open fascinating perspectives for the generation of polar molecules with very large electric dipole moments. Last but not least, the DDI in Rydberg atoms is extremely large [4] and may allow for, e.g., the construction of fast quantum gates [5].

In contrast to the isotropic van-der-Waals-like short-range interactions, the DDI is long-range and anisotropic (partially attractive), and leads to fundamentally new physics in ultra-cold gases, modifying, e.g., the stability and excitations of BECs [6, 7], the properties of Fermi gases [8] and the physics of strongly correlated gases [9]. Time-of-flight experiments in chromium condensates allowed for the first observation of DDI effects in quantum degenerate gases [10], which have been remarkably enhanced recently by means of Feshbach resonances [11]. In addition, the DDI has been recently shown to play an important role in the physics of spinor rubidium BEC [2] and to lead to an observable damping of Bloch oscillations of potassium atoms in optical lattices [12].

The long-range character of the DDI leads to nonlocal nonlinearity in dipolar BECs, similar to that encountered in, e.g., plasmas [13] and nematic liquid crystals [14]. This non-locality leads to novel nonlinear physics in dipolar BECs, including the possibility of obtaining stable two-dimensional (2D) bright solitons [15] and stable 3D dark solitons [16]. In addition, the partially attractive character of the non-local nonlinearity due to the anisotropy of the DDI has remarkable consequences for the stability of dipolar BECs, which may become unstable against collapse in 3D traps, as recently shown in experiments with chromium BECs [17]. In contrast, 2D traps may allow for an instability without collapse, characterized by the formation of a gas of inelastic 2D solitons [18].

Vortices and vortex lines constitute a prominent topic among the fascinating properties of interacting quantum gases. When rotated at a sufficiently large angular frequency, a superfluid develops vortex lines of zero density [19, 20], around which the circulation is quantized due to the single-valued character of the corresponding wavefunction [21]. Quantized vortices constitute indeed one of the most important consequences of superfluidity, playing a fundamental role in various physical systems, such as superconductors [22] and superfluid helium [23]. Vortices and even vortex lattices have been created in alkali BECs in a series of milestone experiments [24]–[26].

Similar to strings, vortex lines are 3D structures that may present transverse helical excitations, which are called Kelvin modes or waves [27]. These excitations were studied for quantized vortices in superfluids by Pitaevskii [28]. Interestingly, the dispersion law for Kelvin modes at the small wave vector q follows a characteristic dependence $\epsilon(q) \sim -q^2 \ln q\xi$,

where ξ is the healing length. Kelvin modes play an important role in the physics of superfluid helium [23, 29], and even of neutron stars [30]. Recently, Kelvin modes were experimentally observed in BEC [31].

The DDI interaction may distort significantly the physics of vortices in dipolar BECs, in particular the critical angular frequency for vortex creation [32]. In addition, dipolar gases under fast rotation develop vortex lattices, which due to the DDI may be severely distorted [33], and may even change the configuration from the usual triangular Abrikosov lattice into other arrangements [34, 35].

In a recent paper [36], we analyzed the case of a dipolar BEC in a 1D optical lattice, and in particular the physics of straight vortex lines perpendicular to the 2D planes defined by the lattice sites. We showed that due to the long-range character of the DDI, different parts of the vortex line interact with each other, and hence the 3D character of the vortices plays a much more important role in dipolar gases than in usual short-range interacting ones. Specifically, we discussed that, interestingly, the DDI may severely modify the Kelvin-wave dispersion, which may even acquire a roton-like minimum. This minimum may touch zero energy for sufficiently large DDI and strong lattices, leading to the instability of the straight vortex line even for those situations in which the BEC as a whole is stable. However, the certainly very relevant question concerning the nature of this instability was not addressed in [36]. In the present paper, we discuss this instability in detail, showing that, interestingly, it has a thermodynamic character, and it is linked to a second-order-like phase transition from a straight vortex line into a helical or snake-like vortex line depending on the dipole orientation.

The structure of the paper is as follows. In section 2, we discuss the effective model that describes a dipolar BEC in a sufficiently strong optical lattice. In section 3, we briefly summarize the main results of [36]. In section 4, we discuss the phase transition from straight to helical vortex lines for the case of dipoles oriented parallel to the vortex line, whereas in section 5, we discuss the transition to a snake-like vortex for dipoles perpendicular to the vortex line. Finally, in section 6, we summarize our conclusions.

2. Dipolar BEC in an optical lattice: effective model

In the following, we consider a dipolar BEC of particles with mass m and electric dipole d (the results are equally valid for magnetic dipoles) oriented in the z-direction by a sufficiently large external field and hence interacting via a dipole–dipole potential: $V_{\rm d}(\vec{r}) = \alpha d^2(1-3\cos^2\theta)/r^3$, where θ is the angle formed by the vector joining the interacting particles and the dipole direction. The coefficient α can be tuned within the range $-1/2 \leqslant \alpha \leqslant 1$ by rotating the external field that orients the dipoles much faster than any other relevant time scale in the system [37]. We consider the dipolar BEC as placed in a 1D optical lattice (see figure 1). At sufficiently low temperatures (and away from shape resonances[2]) the physics of the dipolar BEC is provided by a non-local nonlinear Schrödinger equation (NLSE) of the form

$$\mathrm{i}\hbar\frac{\partial\Phi(\vec{r})}{\partial t} = \left\{-\frac{\hbar^2\nabla^2}{2m} + V_{\rm ol}(z) + g|\Phi(\vec{r})|^2 + \int \mathrm{d}\vec{r'}|\Phi(\vec{r'})|^2 V_{\rm d}(\vec{r}-\vec{r'})\right\}\Phi(\vec{r}), \tag{1}$$

where $g = 4\pi\hbar^2 a/m$, with $a > 0$, is the s-wave scattering length, and $V_{\rm ol}(z) = sE_{\rm R}\sin^2(Q_l z)$ is the 1D optical lattice, where $E_{\rm R} = \hbar^2 Q_{\rm l}^2/2m$ is the recoil energy and $Q_{\rm l}$ is the laser wave vector.

[2] Close to the shape resonances, the form of the pseudpotential must be, in general, corrected (see [38] and references therein).

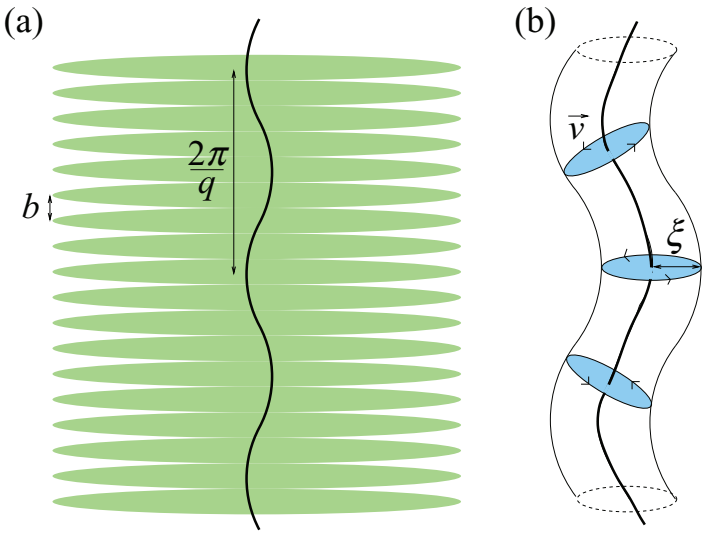

Figure 1. (a) Vortex line in an optical lattice with lattice spacing b. The wave number of the Kelvin mode is q, whereas the corresponding wavelength satisfies $2\pi/q \gg b$. (b) The vortex line has a finite core with healing length ξ and a velocity field $\vec{v}$ perpendicular to the line.

In the tight-binding regime (sufficiently strong lattice), we can write $\Phi(\vec{r},t) = \sum_j w(z - bj)\psi_j(\vec{\rho},t)$, where $b = \pi/Q_l$, $\vec{\rho} = \{x, y\}$ and $w(z)$ is the Wannier function associated with the lowest energy band. Substituting this ansatz into equation (1), we obtain a discrete NLSE. We may then return to a continuous equation, where the presence of the lattice amounts to an effective mass m^* along the lattice direction and for a renormalized coupling constant $\tilde{g}$ [39]:

$$\mathrm{i}\hbar\frac{\partial\Psi(\vec{r})}{\partial t} = \left\{-\frac{\hbar^2\nabla_\perp^2}{2m} - \frac{\hbar^2\nabla_z^2}{2m^*} + \tilde{g}|\Psi(\vec{r})|^2 + \int \mathrm{d}\vec{r}'|\Psi(\vec{r}')|^2 V_\mathrm{d}(\vec{r}-\vec{r}')\right\}\Psi(\vec{r}), \tag{2}$$

where $\Psi(\vec{r}) = \psi_j(\vec{\rho})/\sqrt{b}$ is the coarse-grained wavefunction, $m^* = \hbar^2/2b^2J$ is the effective mass, with $J = \int w(z)[-(\hbar^2/2m)\partial_z^2 + V_\mathrm{ol}(z)]w(z+b)\mathrm{d}z$, and $\tilde{g} = bg\int w(z)^4\mathrm{d}z + g_\mathrm{d}\mathcal{C}$, with $g_\mathrm{d} = \alpha 8\pi d^2/3$ and $\mathcal{C} \simeq \sum_{j\neq 0}|\tilde{w}(2\pi j/b)|^2$, where $\tilde{w}$ is the Fourier transform of $w(z)$. The validity of equation (2) is limited to z-momenta $k_z \ll 2\pi/b$, in which one can ignore the discreteness of the lattice. In addition, note that the single-band model breaks down if the gap between the first and second bands becomes comparable with other energy scales in the problem ($m/m^* \to 1$).

As mentioned above, the partially attractive character of the DDI may lead to different types of instability in a dipolar BEC. We consider first a homogeneous 3D solution $\Psi_0(\vec{r},t) = \sqrt{\bar{n}}\exp[-\mathrm{i}\mu t/\hbar]$, where $\bar{n}$ denotes the condensate density, and $\mu = (g + \tilde{V}_\mathrm{d}(0))\bar{n}$ is the chemical potential, with $\tilde{V}_\mathrm{d}(\vec{k}) = g_\mathrm{d}[3k_z^2/|\vec{k}|^2 - 1]/2$. From the corresponding Bogoliubov–de Gennes (BdG) equations one gets that the energy $\epsilon(\vec{k})$ corresponding to an excitation of wave number $\vec{k}$ fulfills: $\epsilon(\vec{k})^2 = E_\mathrm{kin}(\vec{k})[E_\mathrm{kin}(\vec{k}) + E_\int(\vec{k})]$, where $E_\mathrm{kin}(\vec{k}) = \hbar^2k_\rho^2/2m + \hbar^2k_z^2/2m^*$ is the kinetic energy, and $E_\mathrm{int}(\vec{k}) = 2(g + \tilde{V}_\mathrm{d}(\vec{k}))\bar{n}$. Stable phonons (i.e. low-k excitations) are only possible if $E_\mathrm{int} > 0$ for all directions, i.e. if $2 + \beta(3k_z^2/|\vec{k}|^2 - 1) > 0$, with $\beta = g_\mathrm{d}/\tilde{g}$. If $g_\mathrm{d} > 0$, phonons

with $\vec{k}$ lying on the xy-plane are unstable if $\beta > 2$, whereas if $g_d < 0$, phonons with $\vec{k}$ along z are unstable if $\beta < -1$. Hence, absolute phonon stability demands that $-1 < \beta < 2$.

3. Kelvin-wave instability of a straight vortex line

In this section, we consider a straight vortex line along the z-direction (see figure 1). The corresponding wavefunction is of the form $\Psi_0(\vec{r}, t) = \phi_0(\rho)\exp(i\varphi)\exp[-i\mu t/\hbar]$, where φ is the polar angle on the xy-plane. The function $\phi_0(\rho)$ fulfills

$$\mu\phi_0(\rho) = \frac{\hbar^2}{2m}\left(-\frac{1}{\rho}\partial_\rho\rho\partial_\rho + \frac{1}{\rho^2}\right)\phi_0(\rho) + \bar{g}|\phi_0(\rho)|^2\phi_0(\rho), \tag{3}$$

where $\bar{g} = \tilde{g} - g_d/2$. Note that, due to the homogeneity of Ψ_0 in the z-direction, the DDI just regularizes the local term. The density of the vortex core is given by $|\phi_0(\rho)|^2$, which vanishes at $\rho = 0$ and becomes equal to the bulk density $\bar{n}$ at distances larger than the healing length $\xi = \hbar/\sqrt{m\bar{g}\bar{n}}$ (see figure 1). Note that ξ depends on the DDI.

In the following, we consider Kelvin-wave excitations of the straight vortex line of the form (see figure 1) $\Psi(\vec{r}, t) = \Psi_0(\vec{r}, t) + \chi(\vec{r}, t)\exp[i(\varphi - \mu t/\hbar)]$, where [28] $\chi(\vec{r}, t) = \sum_{l,q}[u_l(\rho)\exp[i(\varphi l + qz - \epsilon t/\hbar)] - v_l(\rho)^*\exp[-i(\varphi l + qz - \epsilon^* t/\hbar)]]$ (as mentioned in section 2, $q \ll 2\pi/b$ in order to justify the validity of the effective model).

Introducing this ansatz into (2) and linearizing in χ, one obtains the corresponding BdG equations:

$$\epsilon u_l(\rho) = \left[\frac{\hbar^2}{2m}\left(-\frac{1}{\rho}\partial_\rho\rho\partial_\rho + \frac{(l+1)^2}{\rho^2} + \frac{m}{m^*}q^2\right) - \mu + 2\bar{g}\psi_0(\rho)^2\right]u_l(\rho) - \bar{g}\psi_0(\rho)^2 v_l(\rho)$$
$$+ \frac{3\beta}{2-\beta}\bar{g}q^2\int_0^\infty d\rho'\rho'\psi_0(\rho')\psi_0(\rho)\left[u_l(\rho') - v_l(\rho')\right]F_l(q\rho, q\rho'), \tag{4}$$

$$\epsilon v_l(\rho) = -\left[\frac{\hbar^2}{2m}\left(-\frac{1}{\rho}\partial_\rho\rho\partial_\rho + \frac{(l-1)^2}{\rho^2} + \frac{m}{m^*}q^2\right) - \mu + 2\bar{g}\psi_0(\rho)^2\right]v_l(\rho) + \bar{g}\psi_0(\rho)^2 u_l(\rho)$$
$$+ \frac{3\beta}{2-\beta}\bar{g}q^2\int_0^\infty d\rho'\rho'\psi_0(\rho')\psi_0(\rho)\left[u_l(\rho') - v_l(\rho')\right]F_l(q\rho, q\rho'), \tag{5}$$

with $F_l(x, x') = I_l(x_<)K_l(x_>)$, where I_l and K_l are the modified Bessel functions, and $x_> = \max(x, x')$, $x_< = \min(x, x')$. For every q we determine the lowest eigenenergy ϵ, which provides the dispersion law discussed below.

The first line at the rhs of equations (4) and (5) is exactly the same as that expected for a vortex in a short-range interacting BEC [28], but with the regularized value $\bar{g}$. Hence, in the absence of DDI (or equivalently from equations (4) and (5) without the last integral term) the dispersion law at low momenta ($q\xi \ll 1$) is provided by the well-known expression $\epsilon(q) = -(\hbar^2 q^2/2m^*)\ln[(m/m^*)^{1/2}q\xi]$. In contrast, the last term at the rhs of both equations is directly linked to the long-range character of the DDI and, as we show below, leads to novel phenomena in the physics of Kelvin modes ($l = -1$) in dipolar BECs. In the following, and in order to isolate the effect of the DDI on the core size with respect to the effect of the integral

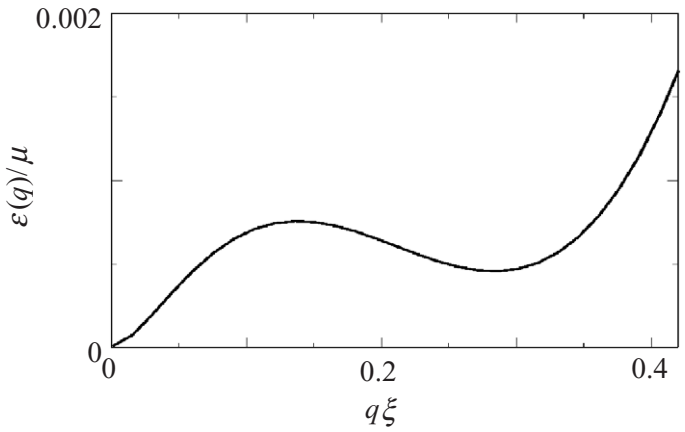

Figure 2. Dispersion $\epsilon(q)$ as a function of $q\xi$ for $m/m^* = 0.143$, and $\beta = -0.8$.

terms in equations (4) and (5), we keep $\bar{g}$ fixed and change the parameter β that is proportional to the dipole–dipole coupling constant.

The integral terms of equations (4) and (5) significantly modify the Kelvin-mode spectrum in a different way depending on whether $\beta > 0$ or $\beta < 0$. The different regimes are summarized in figure 3. As shown in [36], for $\beta > 0$ the excitation energy increases, i.e. the vortex line becomes stiffer against transverse modulations. The opposite occurs for $\beta < 0$, i.e. the Kelvin modes become softer. However, the softening of the Kelvin-wave spectrum never leads to instability in the absence of an additional lattice ($m = m^*$), since destabilization demands $\beta < -1$, for which, as we show in section 2, the whole dipolar BEC is phonon-unstable. Interestingly, an increase of the potential depth of the additional lattice leads to a reduction of the role of the kinetic energy term mq^2/m^* in equations (4) and (5) that enhances the effect of the dipolar interaction on the dispersion law. As a consequence, as shown in figure 2, in addition to the $-q^2 \ln(q\xi)$ dependence at low q, a roton-like minimum eventually appears at intermediate q. For a sufficiently small $(m/m^*)_{\rm cr}$ (thick curve in figure 3) the roton minimum reaches zero energy. For $m/m^* \leqslant (m/m^*)_{\rm cr}$ the energy at the roton becomes negative, and hence the straight vortex line becomes thermodynamically unstable against the formation of a new vortex-line configuration, which we discuss in the following sections.

The intriguing dependence of the dispersion of Kelvin waves on m/m^* and β is explained by the competition of the two processes involved in the inter-site physics, namely tunneling and inter-site DDI. On the one hand, the hopping energy is minimized when vortex cores at neighboring sites are placed right on top of each other. Hence tunneling tends to maintain the vortex line straight. On the other hand, we may obtain an intuitive picture concerning the inter-site DDI by sketching the vortex core as a 1D chain of dipolar holes. Dipolar holes interact in exactly the same way as dipolar particles and hence for $\beta > 0$ attract each other maximally when aligned along the dipole direction, i.e. the z-direction. As a consequence, for $\beta > 0$, DDI and hopping add up in keeping the vortex straight, and the vortex line becomes stiffer. In contrast, for $\beta < 0$ the cores maximally repel each other when aligned along the z-direction. Hence DDI and tunneling compete, and the vortex line becomes softer.

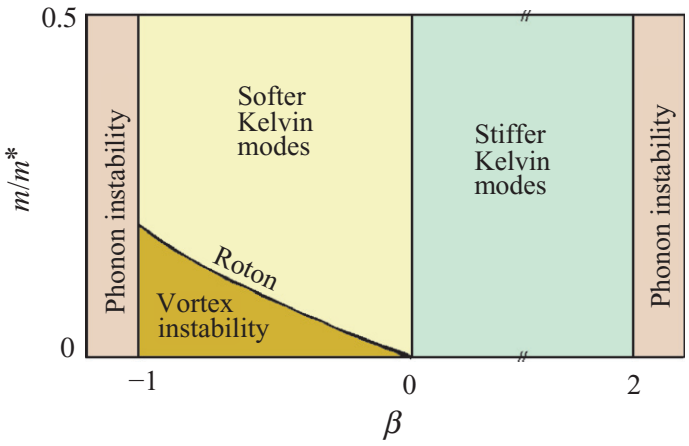

Figure 3. Stable/unstable regimes for straight vortex lines.

4. Helical vortices

From the intuitive picture discussed in the previous section, it becomes clear that when m/m^* becomes sufficiently small, the tunneling cannot balance the DDI any longer, and as a consequence the straight vortex line becomes thermodynamically unstable, as has already been mentioned in our discussion of the Bogoliubov analysis in the previous section. In this section, we show that this instability is related to a transition from a straight vortex to a twisted vortex line. This twisting, which we confirm below numerically, may be expected by analyzing the DDI between vortex cores at neighboring sites. This energy is minimized by laterally displacing the vortices with respect to each other a finite distance on the xy-plane. These lateral displacements between nearest neighbors lead to a twisting of the vortex line. Note that due to the symmetry of the problem, we may expect a helical structure, as we confirm in the following.

In order to determine the new lowest-energy configuration of the vortex line, we have performed fully 3D numerical calculations of the GPE (2). We start our calculations from an initially imposed straight vortex line and let the system evolve in imaginary time. We performed our calculations employing a cylindrical numerical box placed several healing lengths apart from the vortex core to minimize boundary effects. The cylindrical box configuration permits a sufficiently flat density in the region where the vortex core is created, allowing us to avoid unwanted density effects, which will obscure the analysis of the vortex stability. As expected, the imaginary time evolution leads to a ground-state straight vortex line configuration for those values of β and m/m^* lying inside the stable regime of figure 3. In contrast, for those regions within the instability regime a qualitatively new ground state is found, where we observe a departure from the straight form into an helical configuration, as in figure 4.

Hence, at the line $(m/m^*)_{\rm cr}$ there is a phase transition from straight into helical ground-state vortex lines. In order to characterize this phase transition, we have performed an exhaustive analysis of the helical configurations, which may be characterized by a pitch with wave number Q and a radius r_0. We confirmed that the wave number Q is indeed comparable with the minimum $q_{\rm rot}$ in the dispersion law obtained from the Bogoliubov analysis of section 3. For several fixed values of β we performed a large number of 3D numerical simulations for different m/m^*, to analyze the behavior of the amplitude r_0 inside the unstable region and at the transition to the stable region. Our results (for $\beta = -0.8$) are depicted in figure 5.

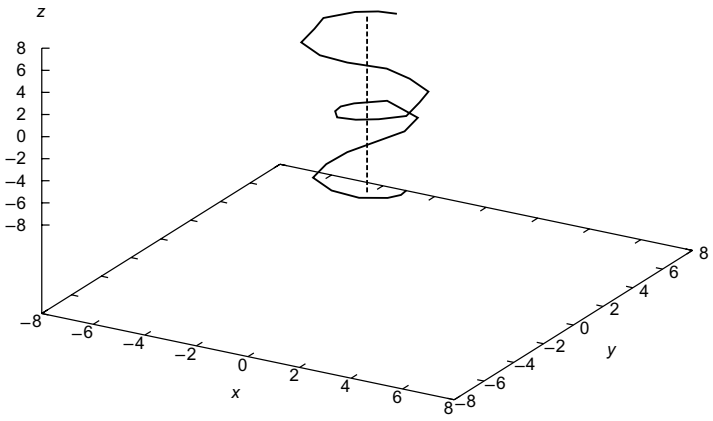

Figure 4. Vortex-line configurations of the ground state for $\beta = -0.8$ and $m/m^* = 0.15$ (straight) and $m/m^* = 0.04$ (helical), respectively. For both cases, the dipole is assumed to be in the z-direction. The unit of length is $\sqrt{2}\xi$.

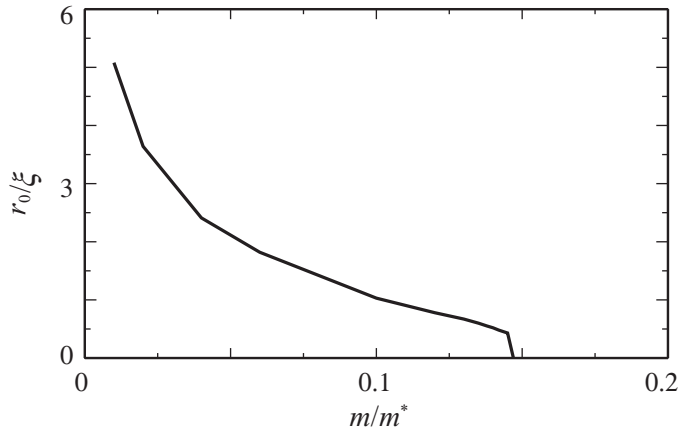

Figure 5. Helix amplitude r_0 (see text) as a function of m/m^* for $\beta = -0.8$.

We observe a gradual decrease of r_0 when m/m^* approaches the stability border $(m/m^*)_{\rm cr}$. For values close to the stability border, $r_0 \ll \xi$ and hence it becomes in practice (both numerically and experimentally) impossible to discern a significant vortex twisting. Our simulations are hence compatible with a second-order-like phase transition from a helical to a straight lowest-energy vortex-line configuration.

Note that inside the instability region an increase of the lattice strength (i.e. a decrease of m/m^*) results in a larger bending, which comes together with a shallower binding energy for the line. If the binding energy becomes lower than other typical energy scales involved in the system (inhomogeneity, boundary effects) then the 3D vortex line breaks into uncorrelated 2D vortices. The latter is, of course, also expected in the absence of DDI if the tunneling becomes sufficiently small. Note that in figure 3, we did not consider any other additional energy scales, and hence the 3D vortex line could be considered all the way down to very small m/m^*. However, in our numerical simulations we do have boundary effects introduced by our finite cylindrical numerical box. As a consequence we have observed (also for the results of the next section) that for very small m/m^* inside the instability regime the boundary effects may completely unbind

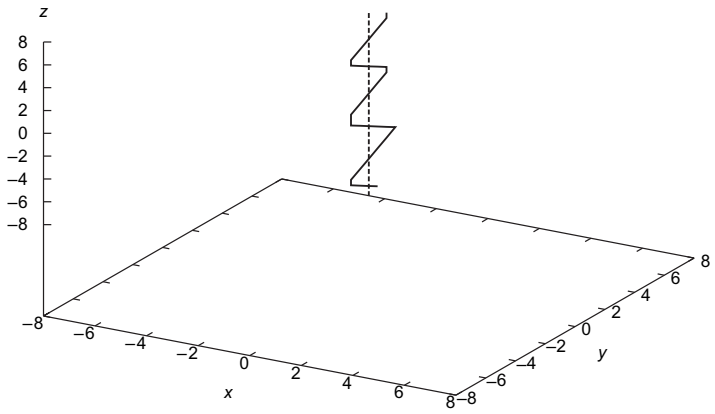

Figure 6. Vortex line configurations of the ground state for $\beta = 1.2$ and $m/m^* = 0.075$ (straight) and $m/m^* = 0.04$ (snake-like), respectively. For both cases the dipole is assumed in the y-direction. The unit of length is $\sqrt{2}\xi$.

the vortex line into uncorrelated 2D vortices at each layer. However, in the present paper, we are more concerned with the phase-transition boundary, where the binding is still dominant even when the vortex is bent.

5. Snake-like vortices

In sections 3 and 4, we have discussed the case where the dipoles are oriented along the z-direction. In that situation, the cylindrical symmetry of the problem largely simplified the Bogoliubov analysis. The helical instability demands that $\beta < 0$, and hence it is necessary to employ the tuning mechanism discussed in section 2. However, the tuning is not strictly necessary to observe the destabilization of the straight vortex line. A perhaps experimentally simpler scenario is offered by the case where the dipoles are oriented perpendicular to the vortex line (and hence also perpendicular to the over-imposed lattice potential). Then the DDI is again repulsive in the z-direction and competes with the kinetic energy in what concerns the stability of the straight vortex line in a similar way as described in previous sections. In this section, we analyze this particular case (orientation along y). We show that the vortex line may also be destabilized in this experimentally less involved case.

As for section 4, we have evolved an initially straight vortex in imaginary time using equation (2) employing similar numerical conditions. However, the analysis in the new configuration is largely handicapped due to the distortion of the density of the condensate induced by the fact that the dipole is now on the xy-plane, and hence breaks the polar symmetry. These density modulations may be reduced (but not fully eliminated) by considering larger numerical boxes. However, the latter may make the 3D numerical simulation prohibitively long.

In spite of these difficulties we observed the departure from the straight vortex line for sufficiently large β (note that in this configuration $\beta > 0$ and hence it may take values up to 2 before entering into the regime of phonon instability discussed in section 2). Due to the broken cylindrical symmetry, for sufficiently large β and small m/m^* the straight vortex line is destabilized into a snake-like configuration on the yz-plane rather than into a helix, as in the previous section, as shown in figure 6. We have analyzed the amplitude of the helix when approaching the stability regime. Our results are compatible with a second-order-like

behavior as in the previous section, although, as mentioned above, a rigorous analysis is largely handicapped by the appearance of strong density modulations in the simulations.

6. Conclusions

In this paper, we have studied the physics of vortex lines in dipolar gases. In particular, we have analyzed in detail the stability of a straight vortex line with respect to Kelvin waves. We have shown that the presence of an additional optical lattice along the vortex line may allow for the observation of a dipole-induced destabilization of the straight vortex line due to the softening of a roton minimum in the Kelvin-wave spectrum. If this occurs the straight vortex-line configuration ceases to be that of minimal energy, and there is a second-order-like phase transition into a helical or snake vortex line, depending on the dipole orientation.

Acknowledgments

We thank P Pedri and R Nath for useful discussions. This work was supported by the DFG (SFB407 and SPP1116) and the ESF (EUROQUASAR).

References

[1] Griesmaier A *et al* 2005 *Phys. Rev. Lett.* **94** 160401
Beaufils Q *et al* 2008 *Phys. Rev.* A **77** 061601
[2] Vengalattore M *et al* 2008 *Phys. Rev. Lett.* **100** 170403
[3] Ospelkaus S *et al* 2008 *Nat. Phys.* **4** 622
Deiglmayr J *et al* 2008 *Phys. Rev. Lett.* **101** 133004
[4] Tong D *et al* 2004 *Phys. Rev. Lett.* **93** 063001
[5] Jaksch D *et al* 2000 *Phys. Rev. Lett.* **85** 002208
[6] Yi S and You L 2000 *Phys. Rev.* A **61** 041604
Góral K, Rzążewski K and Pfau T 2000 *Phys. Rev.* A **61** 051601
Santos L *et al* 2000 *Phys. Rev. Lett.* **85** 1791
[7] Santos L, Shlyapnikov G V and Lewenstein M 2003 *Phys. Rev. Lett.* **90** 250403
Giovanazzi S and O'Dell D H J 2004 *Eur. Phys. J.* D **31** 439
[8] Baranov M A *et al* 2004 *Phys. Rev. Lett.* **92** 250403
[9] Góral K, Santos L and Lewenstein M 2002 *Phys. Rev. Lett.* **88** 170406
Baranov M A, Osterloh K and Lewenstein M 2005 *Phys. Rev. Lett.* **94** 070404
Rezayi E H, Read N and Cooper N R 2005 *Phys. Rev. Lett.* **95** 160404
Büchler H P *et al* 2007 *Phys. Rev. Lett.* **98** 060404
Menotti C, Trefzger C and Lewenstein M 2007 *Phys. Rev. Lett.* **98** 235301
[10] Stuhler J *et al* 2005 *Phys. Rev. Lett.* **95** 150406
[11] Lahaye Th *et al* 2007 *Nature* **448** 672
[12] Fattori M *et al* 2008 *Phys. Rev. Lett.* **101** 190405
[13] Litvak A G *et al* 1975 *Sov. J. Plasma Phys.* **1** 60
[15] Peccianti M *et al* 2004 *Nature* **432** 733
[15] Pedri P and Santos L 2005 *Phys. Rev. Lett.* **95** 200404
Tithonenkov I, Malomed B A and Vardi A 2007 *Phys. Rev. Lett.* **100** 090406
[16] Nath R, Pedri P and Santos L 2008 *Phys. Rev. Lett.* **101** 210402
[17] Lahaye T *et al* 2008 *Phys. Rev. Lett.* **101** 080401

[18] Nath R, Pedri P and Santos L 2008 arXiv:0807.3683
[19] Feynman R P 1955 *Progress in Low Temperature Physics* ed C J Gorter (Amsterdam: North-Holland)
[20] Lishitz E M and Pitaevskii L P 1978 *Statistical Physics II* (Moscow: Nauka)
[21] Onsager L 1949 *Nuovo Cimento* **6** 249
[22] de Gennes P G 1966 *Superconductivity in Metals and Alloys* (New York: Benjamin)
[23] Donelly R J 1991 *Quantized Vortices in Helium II* (Cambridge: Cambridge University Press)
[24] Matthews M R *et al* 1999 *Phys. Rev. Lett.* **83** 2498
[25] Madison K W *et al* 2000 *Phys. Rev. Lett.* **84** 806
[26] Abo-Shaeer J R *et al* 2001 *Science* **292** 476
[27] Thompson W 1880 *Phil. Mag.* **10** 155
[28] Pitaevskii L P 1961 *Sov. Phys.—JETP* **13** 451
[29] Ashton R A and Glaberson W I 1979 *Phys. Rev. Lett.* **42** 1062
[30] Epstein R I and Baym G 1992 *Astrophys. J.* **387** 276
[31] Bretin V *et al* 2003 *Phys. Rev. Lett.* **90** 100403
[32] O'Dell D H and Eberlein C 2007 *Phys. Rev.* A **75** 013604
[33] Yi S and Pu H 2006 *Phys. Rev.* A **73** 061602
[34] Cooper N R, Rezayi E H and Simon S H 2005 *Phys. Rev. Lett.* **95** 200402
[35] Zhang J and Zhai H 2005 *Phys. Rev. Lett.* **95** 200403
[36] Klawunn M *et al* 2008 *Phys. Rev. Lett.* **100** 240403
[37] Giovanazzi S, Görlitz A and Pfau T 2002 *Phys. Rev. Lett.* **89** 130401
[38] Wang D 2007 arXiv:0704.3868
[39] Krämer M, Pitaevskii L and Stringari S 2002 *Phys. Rev. Lett.* **88** 180404